12^{th} International Conference on Fracture Mechanics of Concrete and Concrete Structures
FraMCoS-12
B.L.A. Pichler, Ch. Hellmich, P. Preinstorfer (Eds)

https://doi.org/10.21012/FC12.1224
MS11:1

BEHAVIOUR OF REINFORCED CEMENT CONCRETE UNDER COUPLED CORROSION FATIGUE

VIVEK VISHWAKARMA* **AND SONALISA RAY**†

* PhD. Scholar, Dept. of Civil Engineering,
Indian Institute of Technology Roorkee, Haridwar, India, 247667
e-mail: vivek_v@ce.iitr.ac.in, vivek.200100@gmail.com

†Professor, Dept. of Civil engineering
Indian Institute of Technology Roorkee, Haridwar, India, 247667
e-mail: sonalisa.ray@ce.iitr.ac.in

Key words: Reinforced cement concrete, Fatigue, Corrosion, Coupled corrosion fatigue, Durability

Abstract. This study has investigated the synergistic effects of corrosion and fatigue on lightly reinforced concrete (RCC) structures, with a focus on understanding the coupled deterioration mechanisms in real-world conditions. Concrete beams have been subjected to constant amplitude fatigue loading while submerged in a saline solution to simulate accelerated corrosion. The corrosion kinetics parameters, including corrosion current density (i_{corr}), half-cell potential, and concrete resistivity, have been continuously monitored using a linear polarization resistance (LPR) device during fatigue loading. The study has employed a novel two-beam setup to compare the fatigue life and corrosion rate under coupled loading and staggered loading conditions. The results have demonstrated a significant increase in corrosion current density under fatigue loading compared to control specimens subjected to corrosion alone, highlighting the accelerated degradation due to the combined effects of corrosion and cyclic loading. Pitting corrosion has been found to dominate at the intersection of cracks and the reinforcement bars, with corrosion pits acting as fatigue crack nucleation sites. The study has revealed a clear correlation between corrosion progression and fatigue life, with the coupled corrosion and fatigue loading causing more severe damage and reducing the fatigue life of RCC beams compared to staggered loading conditions. This research has provided critical insights into the coupled corrosion fatigue mechanisms in lightly reinforced concrete flexural members, offering valuable information for understanding the long-term durability and safety of RCC structures subjected to both environmental and loading conditions. The findings have also contributed to the development of better predictive models for the performance and lifespan of concrete infrastructure exposed to aggressive environments.

1 INTRODUCTION

Reinforced Cement Concrete (RCC) structures are the backbone of modern infrastructure, widely used in bridges, buildings, and other critical facilities due to their excellent strength, durability, and versatility. These structures are designed to withstand varied environmental and mechanical loads, ensuring prolonged service life and safety. However, the durability of RCC is often compromised by environmental factors, mechanical stresses, and their combined effects, which can lead to structural degradation and premature failure. Among these factors, corrosion of reinforcing steel and fatigue-induced damage are particularly detrimental.

Corrosion of reinforcement, primarily triggered by chloride ingress or carbonation, weakens the bond between steel and concrete, reduces the cross-sectional area of steel, and accelerates the structural deterioration process. Simultaneously, RCC structures subjected to repeated cyclic loading experience fatigue damage, which manifests as progressive cracking, stiffness degradation, and reduced load-carrying capacity. When these phenomena occur concurrently, their coupled effect—termed as coupled corrosion fatigue—can significantly accelerate structural deterioration, posing serious safety risks and necessitating costly maintenance.

The necessity to study coupled corrosion fatigue arises from the realization that the interaction between these mechanisms is synergistic rather than additive. Corrosion accelerates the initiation and propagation of fatigue cracks by reducing the cross-sectional area of steel (significant mass loss) and creating stress concentration points (pitting). Conversely, fatigue-induced cracking in concrete facilitates the ingress of corrosive agents, thereby accelerating corrosion kinetics. Despite their critical implications for structural health, coupled corrosion fatigue mechanisms remain less explored, particularly under flexural loading conditions.

Recent studies have provided valuable insights into these individual and combined effects. RCC structures are prone to fatigue-induced damage, which compromises their structural integrity over time. Kaplan (1961) [1] provided one of the earliest insights into fatigue behavior in concrete, exploring crack initiation and propagation under cyclic stresses. Building upon this, Bazant and Planas (1998) [2] introduced fracture mechanics models, emphasizing the quasi-brittle nature of concrete and its response to fatigue. Experimental studies highlighted critical factors influencing fatigue life, including stress amplitude, loading frequency, and environmental conditions. Recently, numerical approaches, by Wang et al. (2019) [3], a FE model have been developed to predict fatigue crack growth and stiffness degradation, offering improved understanding of RCC performance under fatigue loading.

Parallel to fatigue, corrosion of reinforcing steel poses another significant durability concern for RCC structures. Initiated by chloride ingress or carbonation, corrosion reduces the cross-sectional area of reinforcement and weakens the bond between steel and concrete, ultimately compromising the load-bearing capacity of RCC. Chernin and Val (2003) [4] demonstrated that corrosion-induced cracking in concrete accelerates structural degradation, while Andrade and Alonso (2001) [5] detailed the electrochemical processes driving corrosion. Numerical frameworks, such as those developed by Vu and Stewart (2005) [6], have been instrumental in probabilistically modeling the progression of corrosion-induced damage, integrating chloride diffusion and crack propagation effects.

In practical scenarios, corrosion and fatigue often occur simultaneously, interacting in ways that significantly exacerbate structural deterioration. Early investigations treated these mechanisms as additive, highlighting their individual contributions to damage. For instance, Zhang et al. (2020) [7] demonstrated that corrosion pits on reinforcement serve as stress concentrators, thereby accelerating fatigue crack growth. Similarly, Nguyen et al. (2018) [8] showed that cyclic loading facilitates crack opening in concrete, enhancing the ingress of aggressive agents and intensifying corrosion kinetics. Molina et al. (1993) [9] integrated these effects into predictive models, albeit without fully addressing their synergistic interactions.

Some studies have moved beyond additive effects to emphasize the synergistic coupling between corrosion and fatigue. Bertolini et al. (2013) [10] experimentally established that fatigue-induced cracking accelerates chloride ingress, amplifying corrosion rates and further weakening the reinforcement. Conversely, corrosion-induced pits and cross-sectional loss significantly reduce the fatigue life of reinforcement, as demonstrated by Du et al. (2015) [11]. Numerical investigations, such as those by Li et al. (2020) [12], have coupled electrochemical corrosion models with fatigue crack propagation frameworks, providing a more comprehensive understanding of their interactive effects. These findings underscore the need for a coupled corrosion fatigue approach to predict the long-term performance of RCC structures under real-world loading and environmental conditions.

In summary, while extensive research has been conducted on the individual effects of fatigue and corrosion in RCC, their coupled behavior remains less explored, particularly under flexural loading conditions. This study addresses these gaps by investigating the synergistic interactions between corrosion and fatigue through experimental observations.

This study has focused on quantifying the acceleration of corrosion kinetics under ongoing fatigue cycles and examining its implications for structural integrity. Through coupled corrosion and fatigue experiments, it has aimed to contribute to a deeper understanding of the synergistic effects of these mechanisms. A novel experimental setup has been introduced, wherein lightly reinforced RCC beam specimens have been tested under constant amplitude fatigue loading while submerged in a saline solution and subjected to accelerated corrosion. Corrosion kinetic parameters, such as corrosion current density (i_{corr}), along with visual observations of metal deterioration, have been recorded using a linear polarization resistance (LPR) device during the application of fatigue loading. A quantitative comparison has subsequently been conducted under three different loading conditions.

2 EXPERIMENT PROGRAM

2.1 Material properties

The concrete beams have been cast using 43-grade ordinary Portland cement, with the mix design prepared as per the guidelines of IS 10262:2009. Locally available river sand, with a specific gravity of 2.59, has been used as fine aggregate, while coarse aggregate with a maximum size of 10 mm has been incorporated. The details of the mix proportions and the properties of the materials used in concrete preparation have been summarized in Table 1. The 28-day average cube compressive strength of standard-sized specimens has been measured as 38 N/mm^2. Deformed bars of grade Fe 550SD have been used as reinforcement, with a tested yield strength of 653 N/mm^2. Concrete beams with dimensions 1000 mm X 200 mm X 120 mm have been cast and cured for 28 days. The reinforcement ratio has been designed in accordance with the criteria outlined by Bosco and Carpinteri (1992) [13]. A notch of 30 mm length has been provided at the mid-span of the beam bottom. A clear cover of 500 mm has been provided to the rebar. The beams have been tested in an inverted position, as shown in Figure 1.

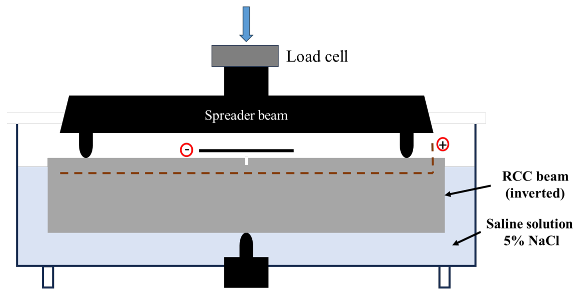

Figure 1: Schematic for the experimental setup.

Table 1: Details of concrete mix and material properties

w/c , (mm)	0.45
Mix proportion	1:1.74:2.2
f_{ck}	38 N/mm^2
Tensile strength (ft)	3.7 N/mm^2
Poisson's ratio (ν)	0.2
Young's Modulus (E)	33980 N/mm^2

2.2 Test setup

The beam specimens have initially been tested under displacement-controlled monotonic loading to assess their flexural capacity. The loading rate has been maintained at 0.005 mm/sec deflection at the center of the beam. The beam specimens have subsequently been tested under three different loading conditions to evaluate their behavior under fatigue loading.

1. Under constant amplitude fatigue loading without impressed current: Plain fatigue loading.
2. Under impressed current and then constant amplitude fatigue loading: Staggered loading.
3. Under simultaneous impressed current and constant amplitude fatigue loading: Coupled loading.

The beams have been tested under fatigue loading of constant amplitude at a load ratio of 0.5 and a frequency of 2 Hz until failure. Initially, the beams have been tested under plain fatigue loading to assess their fatigue limit. A two-beam setup has been created to compare the coupled effects of fatigue and corrosion, as shown in Figure 2. In the first setup, three coupled beam specimens have been tested under the combined loading of fatigue and impressed current, simulating coupled loading conditions. In the second setup, a control beam has been subjected to impressed current only and then tested under fatigue loads, simulating staggered loading conditions. The control beam has been exposed to the same corrosion duration and current density as the coupled beams. Both setups have been maintained in the same environmental conditions to minimize deviations in corrosion readings due to temperature and humidity. This approach has enabled the evaluation of both the synergistic and additive effects of the two mechanisms.

Figure 2: Schematic for the experimental setup.

To ensure the feasibility of the experimental duration, corrosion has been accelerated using controlled techniques, enabling the simulation of long-term deterioration processes within a manageable time frame. Both beams have been subjected to accelerated corrosion using the impressed current technique. A current density of 700 $\mu A/cm^2$ has been applied to both beam specimens for similar time intervals. A stainless steel plate has been used as the cathode, with wet foam placed between the cathode and the beam surface to ensure proper electrical continuity. A 5% $NaCl$ solution has been used as the electrolyte.

In the case of the coupled loading, impressed current and fatigue loading have been initiated simultaneously. Fatigue loading has been intermittently paused at predefined cycles to record corrosion measurements. During these intervals, the beam specimens have been rested for 30 minutes before taking the corrosion measurements to dissipate any residual static charge within the concrete generated by the impressed current. This resting period has been essential for developing and stabilizing the micro-cell activity within the concrete and ensuring accurate electrochemical measurements.

A linear polarization resistance (LPR) device from Giatek Scientific Inc., capable of measuring i_{corr}, concrete resistivity, and corrosion potential, has been utilized to monitor the kinetics of the electrochemical reactions. Corrosion measurements have been taken along the rebar face of the concrete beam at intervals of 150 mm.

3 EXPERIMENTAL RESULTS AND DISCUSSIONS

The beam specimens have been initially tested under deflection-controlled monotonic load, with the mean peak load capacity of three beam specimens found to be 33.6 kN. The load versus deflection plot has been presented in Figure 3.

The failure of the beams has been characterized by yielding, followed by the fracture of the reinforcement, culminating in a ductile failure mode. Subsequently, the beam specimens have been tested under the two-beam setup described earlier, subjected to a fatigue load with a load ratio of 0.5. The fatigue-induced failure of the beams has been attributed to the fatigue failure of the reinforcement bars. Notably, no yielding of the reinforcement has been observed during the fatigue tests, and the failure has exhibited a brittle nature.

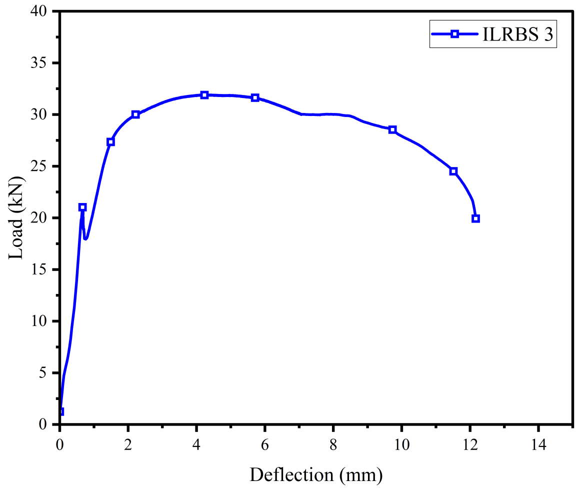

Figure 3: Load versus deflection for the beam specimen ILRBS-3.

The progression of fatigue failure has followed three distinct stages: an initial phase of stiffness degradation, a stable phase during which the beam has behaved almost elastically due to the fatigue response of the reinforcement, and a final phase of sudden brittle failure.

Maximum and minimum deflections per load cycle have been presented in Figures 4 and 5, and the fatigue life of different beam specimens has been shown in Table 2. The average reduction in fatigue life of beam specimens under coupled loading conditions has been recorded as 13% with respect to the staggered loading condition and 27% with respect to plain fatigue loading.

Figures 4 and 5 have revealed distinct trends in the deflection behavior of the coupled beam compared to the control beam during the second stage of the fatigue response. In the coupled beam specimens, both the maximum and minimum deflections have shown a gradual increase as the fatigue cycles have progressed. Conversely, in the control beam, the second-stage fatigue response has remained predominantly elastic, with only a slight increase in the minimum deflection observed as the number of cycles has increased.

The deflection range, defined as the difference between the maximum and minimum deflections, showed a clear increasing trend with the progression of fatigue cycles in the coupled beam specimens.

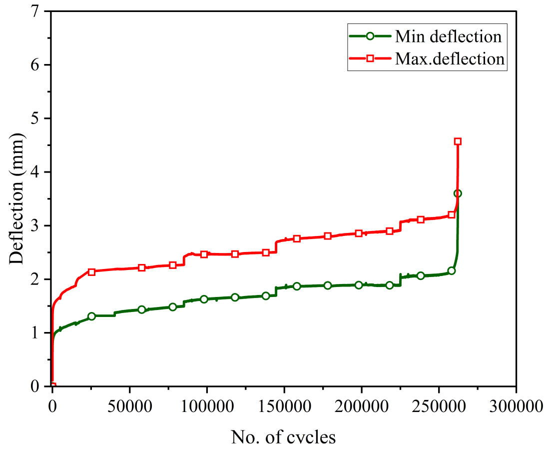

Figure 4: Max. and min. deflection curve of ILRBC5-2 under coupled loading condition.

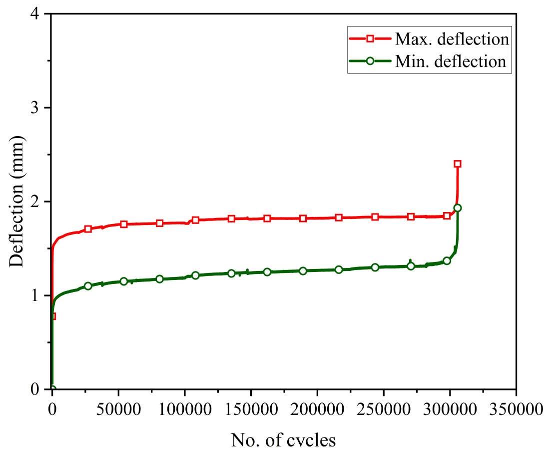

Figure 5: Max. and min. deflection curve of ILRBC5-2 control specimen.

In contrast, the control beam specimens have exhibited only a slight decrease in the deflection range over the same period. These observations have indicated that stiffness degradation is considerably more pronounced in the coupled beam, highlighting the accelerated structural deterioration resulting from the combined effects of fatigue and corrosion.

Table 2: Number of cycles to failure for different beam specimens.

S.No.	Loading condition	Specimen	No. of cycles to failure N_f
1	Coupled	ILRBC5-1	262160
2	Coupled	ILRBC5-2	286805
3	Coupled	ILRBC5-3	249698
4	Control	ILRBC5-C	305682
5	Plain fatigue	ILRBC5-P	364577

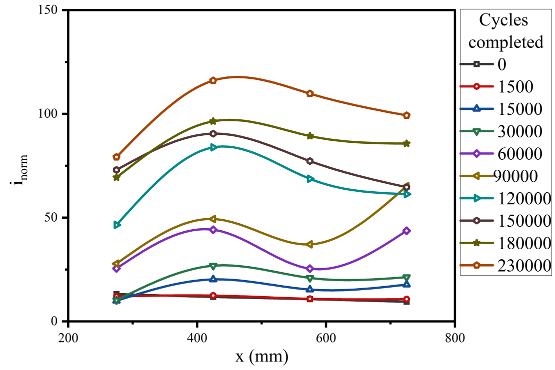

Figure 6: Variation i_{norm} in coupled specimen with the number of cycles completed

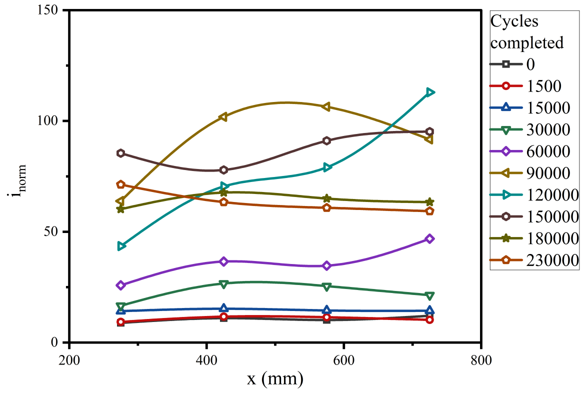

Figure 7: Variation i_{norm} in control specimen with the number of cycles completed

The i_{corr}, concrete resistivity, and half-cell potential have been recorded at regular intervals of fatigue cycles. The LPR device used for this purpose has offered a non-destructive approach to measuring the corrosion rate, eliminating the need for a hard electrical connection with the rebar. Instead, it has employed a patented circuit to estimate the corrosion rate directly from the concrete surface. This method has proven to be both convenient and capable of providing real-time measurements during testing. However, the corrosion rate determined using this approach has been sensitive to the concrete resistivity. To address this limitation, this study has utilized the normalized corrosion rate, i_{norm}, to account for variations in resistivity and ensure more reliable assessments.

$$i_{norm} = i_{corr} \times R \tag{1}$$

where R has been the concrete resistivity in $Kohm.cm$ and i_{corr} has been the corrosion rate in $\mu A/cm^2$.

Figures 6 and 7 have shown the variation of normalized corrosion rate with the cycles completed. For both types of specimens, the corrosion rate has been higher in the central part with respect to the ends of the beam.

However, the coupled beam has shown a higher increase in corrosion rate with the completed cycles than the control specimen. As the loading cycles have elapsed, the corrosion rate at the center of the beam has increased linearly until the failure of the beam, as shown in Figure 8.

This behavior has been attributed to the fatigue-induced crack at the center of the beam, which has enhanced the availability of the electrolyte, thereby increasing the corrosion rate. Additionally, the corrosion products formed have been able to ooze out through the crack, continuously exposing fresh metal to the corrosive environment and sustaining the corrosion process.

In contrast, for the control specimen, the corrosion rate has initially risen but has subsequently declined. This has occurred because the corrosion products formed have not been able to escape from the concrete, instead creating a partial barrier that has slowed down the corrosion process, resulting in a reduced corrosion rate over time.

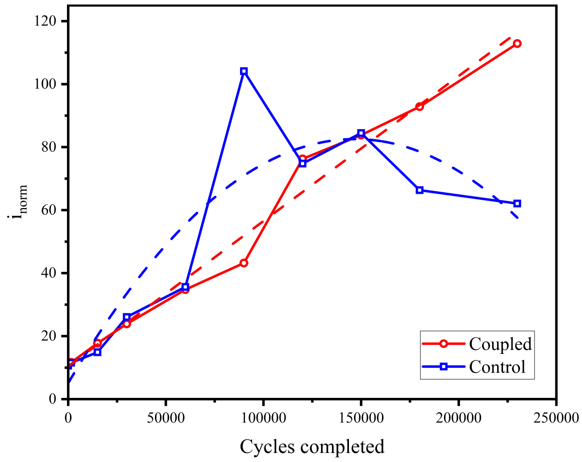

Figure 8: Comparison of i_{norm} in coupled and control beam at the center of the beam with the number of cycles completed

After the fatigue test, the rebars have been extracted from the beam specimens for visual observations. Figure 9 shows the extracted rebars from the beam specimens. Loose rust has been cleaned from the rebars. The picture shows the pit geometry and distribution of the corrosion in two different load cases. In the case of staggered loading, the pits have been few but larger in size. The corrosion pits are scattered relatively farther from the center of the beam. In the case of coupled loading, the pits have been smaller in size and concentrated around the failure zone. In coupled loading specimens, the ribs have also been severely distorted by pitting and slipping, which has justified the higher deflection in coupled loading.

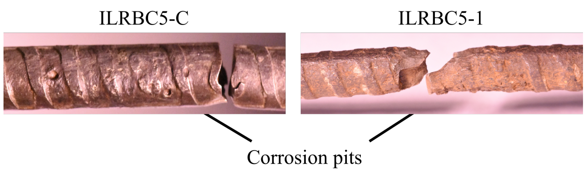

Figure 9: Extracted rebar from the failed beam specimens

4 CONCLUSIONS

The synergistic effect of coupled corrosion fatigue has been investigated in this study using a new experimental setup and compared with the traditional staggered approach. The lightly reinforced RCC beams have been tested under three different loading conditions, and corrosion kinetics parameters, like the corrosion rate, have been assessed.

- A new two-beam setup has been employed to compare the fatigue life and corrosion rate under different loading conditions of coupled loading and staggered loading.

- A significant reduction in fatigue life of the RCC beam has been observed under different loading conditions. A 13% reduction in fatigue life has been observed in coupled loading when compared to staggered loading, and a 27% reduction in fatigue life has been observed when compared to plain fatigue loading.

- In the case of staggered loading, the control beam has shown an increase in the normalized corrosion rate in the initial cycles. Subsequently, the normalized corrosion rate has fallen with an increasing number of cycles.

- In the case of coupled loading, the normalized corrosion rate has linearly increased with the number of cycles completed.

- Visual observations for the pitting characteristics on the rebar have been made. It has been found that the pitting characteristics have been different in the two different loading conditions. In coupled loading, the pits have been concentrated near the crack and smaller in size, whereas in staggered loading, the corrosion pits have been larger in size and scattered around the center of the beam.

REFERENCES

[1] M.F. Kaplan. Crack propagation and the fracture of concrete. *Journal of the American Concrete Institute*, 58:591–610, 1961.

[2] Z.P. Bažant and J. Planas. *Fracture and Size Effect in Concrete and Other Quasibrittle Materials*. CRC Press, 1998.

[3] Jie Wang, Wei Jiang, and Qi Wang. Experimental and numerical evaluation of fatigue crack growth rate based on critical plastically dissipated energy. *International journal of fatigue*, 118:87–97, 2019.

[4] L. Chernin and D.V. Val. Long-term performance of corrosion-damaged reinforced concrete beams. *ACI Structural Journal*, 100(4):408–417, 2003.

[5] C. Andrade and C. Alonso. Corrosion rate monitoring in the laboratory and onsite. *Construction and Building Materials*, 15:315–321, 2001.

[6] K. Vu and M.G. Stewart. Structural reliability of concrete bridges including improved chloride-induced corrosion models. *Structural Safety*, 27:241–267, 2005.

[7] K. Zhang et al. Stiffness degradation for fatigue of reinforced concrete beams after electrochemical rehabilitation. *Engineering Structures*, 220:110998, 2020.

[8] M.N. Nguyen et al. Reliability of reinforced concrete structures subjected to corrosion, climate change, and cyclic loading. *International Journal of Concrete Structures and Materials*, 12:1–14, 2018.

[9] FJ Molina, C Alonso, and C Andrade. Cover cracking as a function of rebar corrosion: Part 2—numerical model. *Materials and structures*, 26:532–548, 1993.

[10] L. Bertolini et al. Effect of reinforcement corrosion on the fatigue strength of reinforced concrete beams. *Cement and Concrete Research*, 54:85–95, 2013.

[11] X. Du et al. Coupled effects of reinforcement corrosion and cyclic loading on performance of rc beams. *Engineering Structures*, 104:195–207, 2015.

[12] W. Li et al. Numerical investigation of coupled corrosion and fatigue in reinforced concrete structures. *Structural Concrete*, 21(5):1620–1634, 2020.

[13] Crescentino Bosco and Alberto Carpinteri. Fracture mechanics evaluation of minimum reinforcement in concrete structures. In *Applications of fracture mechanics to reinforced concrete*, pages 347–378. CRC Press, 2018.